Studies of Air-Coupled Capacitive Ultrasonic Transducers with TiO_2 High-*k* Dielectric Backplate Electrode Coatings

William M. D. Wright and Sean G. McSweeney

Department of Electrical and Electronic Engineering, University College Cork, Ireland
bill.wright@ucc.ie

***Abstract*— Capacitive ultrasonic transducers for operation in air typically consist of a rigid backplate electrode and a movable flexible membrane electrode. The backplate is often contoured or textured to modify the frequency response and sensitivity of the device, and the membrane electrode is typically a metallized dielectric polymer film. The compliance of the air in the gap between the two electrodes provides the restoring force for the membrane. The sensitivity of these devices would be increased if the dielectric constant *k* of the membrane electrode could be increased, but suitable high-*k* materials are often not found in membrane form. Also, most polymer membrane materials are relatively fragile; metal foils may be used as membrane electrodes in harsh environments, but lack the additional dielectric effect of the polymer membranes. Hence, the inclusion of a high-*k* dielectric layer on the backplate electrode should increase the device capacitance and hence its sensitivity. Earlier work investigated the use of HfO_2 high-*k* layers in this regard. This latest work has investigated the effect of using TiO_2 high-*k* layers on the backplate electrode of an air-coupled capacitive ultrasonic transducer for enhanced operation in air.**

A series of reproducibly textured backplate electrodes were micromachined, consisting of a regular array of small pits etched into a silicon substrate, and then electroded with platinum. A layer of TiO_2 high-*k* dielectric material was then deposited to different depths on a selection of backplates. A metallized 5 µm PET membrane electrode was then used to produce a range of capacitive ultrasonic transducers for operation in air. These devices were then tested and characterized as transmitters and receivers, and the effects of the TiO_2 layers investigated.

The capacitance of the devices was modeled to include the capacitances of the active pits and the parasitic capacitance of the intermediate areas, and measurements were in good agreement with the predicted values. The effect of TiO_2 high-*k* layer thickness on device sensitivity and fractional bandwidth was investigated experimentally, and both were seen to increase with the TiO_2 layer thickness, as expected. These latest devices with a TiO_2 layer were less sensitive than earlier devices with equivalent layers of HfO_2 high-*k* dielectric due to the lower breakdown voltage and dielectric characteristics of TiO_2.

***Index Terms*— High-*k* dielectric, capacitive ultrasonic transducer, air coupled ultrasound, titanium dioxide, silicon backplate electrode**

This work was supported by a Government of Ireland IRCSET scholarship under the Embark Initiative, SFI Research Frontiers Program grant 11/RFP.1/ECE/3119, and NAP 225 from the Tyndall National Institute, UCC.

I. Introduction

Traditional applications of air-coupled ultrasound were restricted to range finding and object location, due to the fact that the majority of air-coupled ultrasonic transducers were piezoelectric, and had a narrow bandwidth in order to make them sufficiently sensitive. Capacitive ultrasonic transducers (CUTs) are an exception, as they tend to have a high coupling efficiency and a relatively high bandwidth. More recent air-coupled applications have included non-contact material inspection [1-3], and air-coupled ultrasonic transmission of data [4].

CUTs typically consist of one rigid backplate electrode covered by a movable frontplate electrode or membrane, usually a metal foil or metallized polymer film. The sensitivity and frequency response of a CUT is influenced largely by (a) the mechanical and dielectric properties of the membrane, and (b) the air gap between the two electrodes, which is principally determined by the surface properties of the backplate [5, 6]. Devices operating at frequencies of up to 2-3 MHz have been reported [6, 7], and also operation at elevated temperatures in excess of 800°C [8].

One issue associated with many CUTs is a certain level of variability between nominally identical devices; CUTs typically require manual assembly, leading to slight differences in the membrane clamping and the inclusion of dirt. Often the backplate electrodes have inter-device variations due to the method of manufacture. Using standard lithographic techniques from the semiconductor industry, it is possible to produce a range of backplate structures in a highly repeatable manner [7, 9].

In order to further increase CUT sensitivity, it is usually desirable to increase the device capacitance. Suitable high-*k* frontplate electrode materials in a convenient membrane form are limited, and so the potential for adding dielectric layers to the surface of the backplate was investigated. Previous work [10] used HfO_2 as the high-*k* dielectric material, and the current work is an extension of this, investigating TiO_2 layers deposited on an etched silicon backplate electrode.

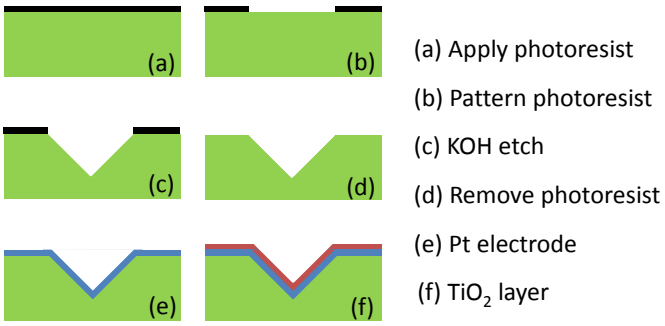

Fig. 1. Schematic of fabrication process steps.

II. Design, Modeling and Characterization

A. Fabrication

A series of (100) silicon wafers were KOH etched, Pt electroded and coated with a layer of TiO_2 high-*k* dielectric, as shown schematically in Fig. 1. An initial photoresist layer (a) applied to the bare silicon substrate was then patterned (b) with a regular grid of 40 µm square holes with 80 µm center spacing using a UV source. The self-limiting etch (c) produced pyramidal pits with sloping sides at an angle of 54.736°. The photoresist was removed (d) and the Pt electrode deposited (e). Finally the high-*k* TiO2 layer was deposited (f) to a thickness of 200 nm, 400 nm, 600 nm, 800 nm or 1000 nm across the entire wafer. The wafer was then diced into squares of side 16 mm for incorporation into screened transducer housings with a 12 mm diameter aperture. A more detailed description of the device structure and geometry has been described in previous work [10].

B. Device Modeling

The pits were symmetric square pyramids of edge length γ, and sidewall incline α. A schematic cross-section of a pit in an assembled device can be seen in Fig. 2. Similar pitted backplate features were modeled previously [9] using a standard equivalent circuit model. A dc bias is applied between the Al electrode on the membrane and the Pt electrode on the backplate. When operating as a transmitter, an ac signal is superimposed to generate ultrasound in the surrounding air. When operating as a receiver, an ultrasonic wave causes the membrane to move and the resulting charge variation is detected and amplified.

For the pitted backplate structure used in this work with N pits, the active capacitance is given by the sum of N pit capacitances C_A in parallel with the capacitance of the region between devices C_P, which is considered parasitic, given by

$$C_P = \frac{\varepsilon_0 \varepsilon_m \varepsilon_k \left(d^2 - N\gamma^2\right)}{\left(t_m \varepsilon_k + t_k \varepsilon_m\right)}, \quad (1)$$

$$C_A = \frac{8\varepsilon_0 \varepsilon_m \varepsilon_k \gamma^2 \ln\left|\sec\left(\frac{\gamma}{2} - \frac{\pi}{2}\right)\right|}{\varepsilon_m \varepsilon_k \gamma^2 + 8\left(t_m \varepsilon_k + t_k \varepsilon_m\right) \ln\left|\sec\left(\frac{\gamma}{2} - \frac{\pi}{2}\right)\right|}, \quad (2)$$

where ε_0 is the permittivity of free space, ε_k and ε_m are the relative permittivities of the membrane and high-*k* layer, respectively, t_k and t_m are the thicknesses of the membrane and high-*k* layer, respectively, γ is the pit edge length, and d is the edge length of the overall backplate. The active capacitance increases with high-*k* layer thickness, but the parasitic capacitance decreases. Due to the geometry of the devices used in this study, the parasitic capacitance between the pits was significantly larger than the active pit capacitance, resulting in an overall decrease in device capacitance as the high-*k* layer thickness increased. The parameters used in this study are shown in Table I.

C. Experimental Layout

The experimental apparatus used in this work is shown schematically in Fig. 3. A high-*k* TiO_2 CUT was used as a transmitter, driven by a 12.5 µJ impulse from a Panametrics 5800 combined with a dc bias of up to 300 V from a Delta Elektronika SM 3004-D power supply. The air-coupled ultrasound was detected using a second CUT as a receiver, with signals amplified using a Cooknell CA6/C charge sensitive amplifier with a SU1/C 100 V biasing unit, and an additional 20 dB of gain from a Princeton 5113. MATLAB© was used for overall system coordination, data collation from the Tektronix TDS 200 series oscilloscope, and processing.

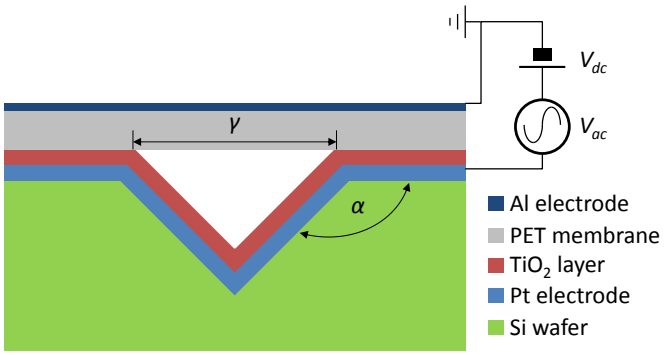

Fig. 2. Schematic section of assembled pit geometry.

TABLE I
Parameters of The TiO_2 High-*K* Device

PARAMETER	VALUE
Pit angle, α	125.264°
Pit center spacing, β	80 µm
Pit edge length, γ	40 µm
Backplate edge length, d	16 mm
Sound speed in air, c	343 ms^{-1}
Density of air, ρ_0	1.2251 kgm^{-3}
Permittivity of free space, ε_0	8.854 pF/m
Permittivity of TiO_2, ε_k	80
Permittivity of PET, ε_m	3.4
Receiver frequency, f_0	250 kHz
Receiver Q factor	2
Number of pits, N	2704

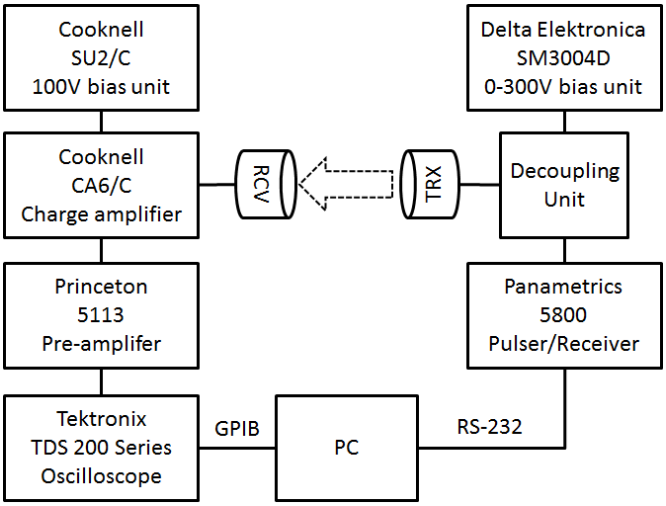

Fig. 3. Schematic diagram of the experimental apparatus.

III. Results and Discussion

The capacitance of each high-*k* TiO_2 CUT was obtained from the RC time constant curve for an applied step response of 20 V with a constant dc bias of 100 V, measured three times and averaged. The theoretical capacitance of each device with a different TiO_2 layer thickness was calculated using (1) and (2); this is plotted in Fig. 4 along with the experimentally measured capacitance. The difference between the calculated and measured capacitance for each thickness of TiO_2 layer was less than 6.6%, but this still highlights the inherent variability of CUTs due to manual assembly. Typical ultrasonic signals propagated through 40 mm of air, and their corresponding frequency spectra, are shown in Fig. 5, where it can be seen that the thicker TiO_2 layer has produced a more sensitive device. Fig. 6 shows the variation in device sensitivity with TiO_2 layer thickness, and a strong linear correlation is seen, as expected. It can be seen that the overall device sensitivity for a high-*k* TiO_2 layer 1000 nm thick is nearly four times that of a device without a layer of TiO_2. Fig. 7 shows the measured fractional bandwidth plotted against TiO_2 layer thickness, and again an overall increasing trend is evident, as expected. The increase in active capacitance C_A produces a greater charge for the same bias

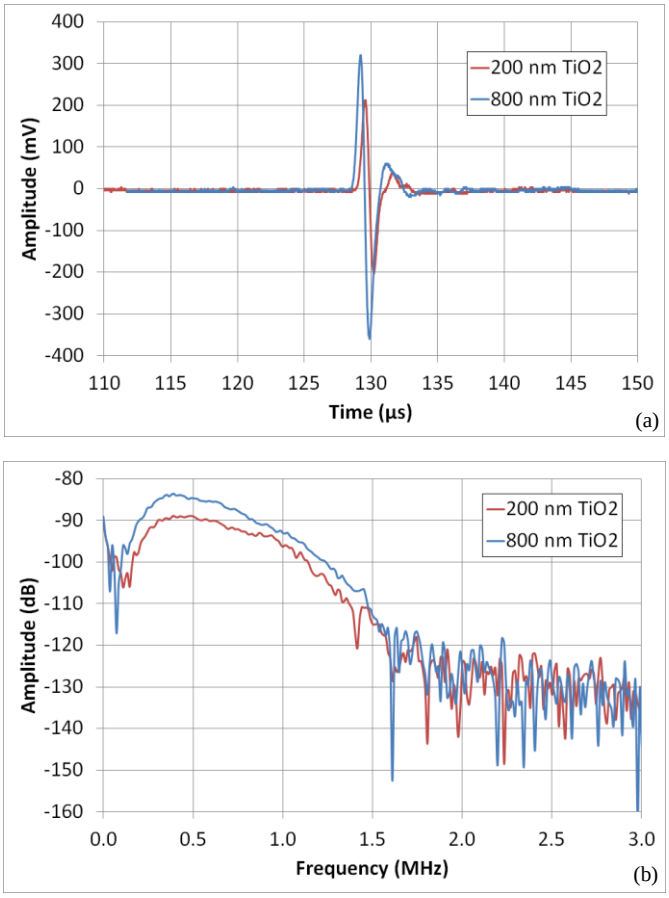

Fig. 5. Time domain impulse (a) and frequency domain (b) responses of 200 nm and 800 nm thickness TiO_2 layer devices.

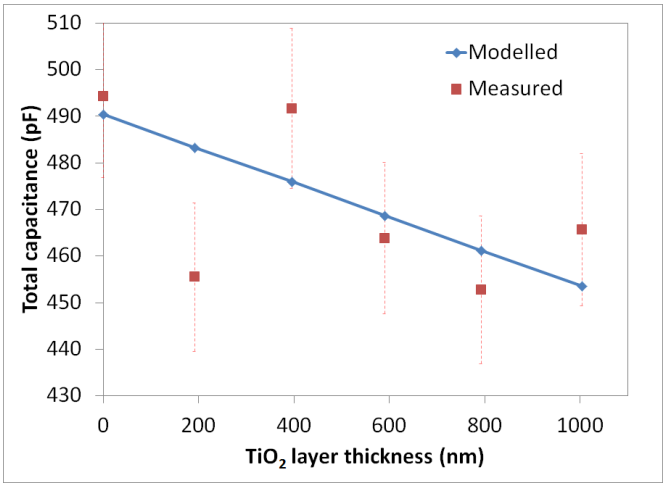

Fig. 4. Variation in modeled and measured total device capacitance vs. TiO_2 layer thickness.

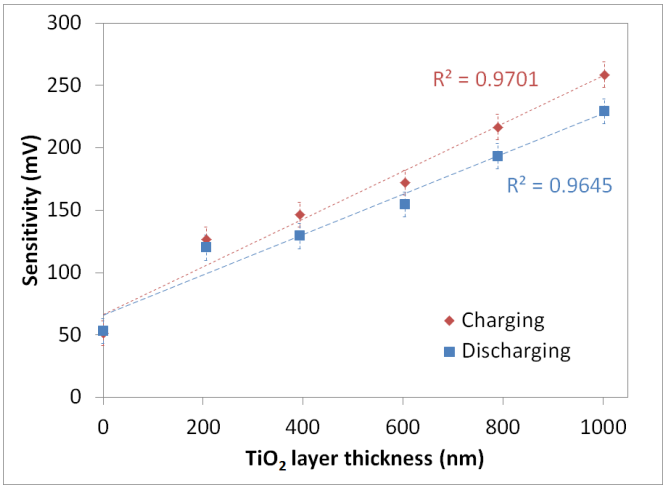

Fig. 6. Sensitivity (received peak-to-peak signal amplitude) vs. TiO_2 layer thickness, for bias charging and discharging cycles.

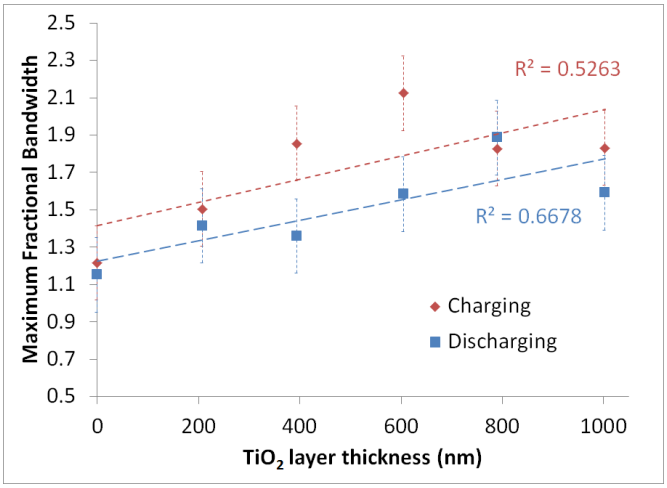

Fig. 7. Fractional bandwidth vs. TiO_2 layer thickness, for bias charging and discharging cycles.

voltage, resulting in an increase in electrostatic force and greater damping of the membrane and a corresponding increase in the fractional bandwidth.

Fig. 8 shows five successive dc bias charging and discharging sweeps up to 300 V in 256 steps for the 200 nm TiO_2 layer device as a representative example. The initial portion of the first charging cycle of all devices was always slightly different, which was attributed to excess air being forced out from between the PET membrane and backplate. It can be seen in Fig. 8 that the sensitivity decreases slightly with successive charge-discharge cycles, which was attributed to dielectric charging. There was little variation in either the sensitivity (maximum peak-to-peak voltage) or the bias voltage at which this occurred, between successive bias charging and discharging cycles, for all the different TiO_2 layers. However, there was significant variation between successive charge-discharge cycles for the device with no TiO_2 layer, indicating that the phenomenon was most likely due to charge injection and polarization in the PET membrane and not the high-*k* layer.

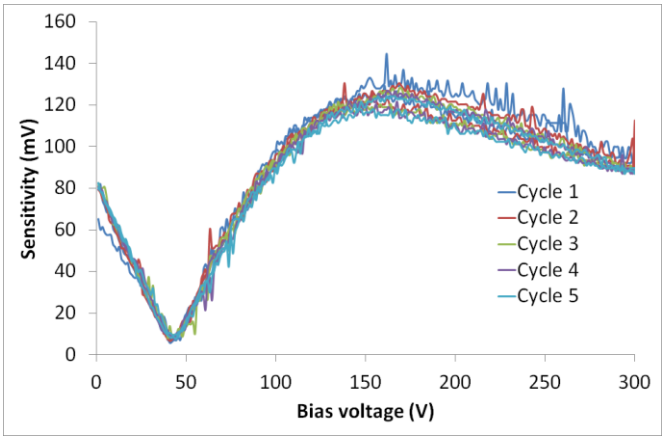

Fig. 8. Sensitivity vs. bias voltage, for a 200 nm thickness TiO_2 dielectric layer for 5 successive bias charge/discharge cycles up to 300 V.

IV. Conclusions and Future Work

As can be seen from the results presented in this work, there are significant improvements in the performance of the CUTs with a TiO_2 high-*k* dielectric layer that depend on the layer thickness. A four-fold increase in sensitivity and a near two-fold increase in fractional bandwidth were observed when comparing devices with no TiO_2 layer and a TiO_2 layer 1000 nm thick.

Variation in total device capacitance was as expected to within 6.6%, and the results showed that despite a decrease in the total capacitance of the device, the capacitance of the active area incorporating the pits was increasing, with a corresponding increase in both the sensitivity and fractional bandwidth of the devices correlated to the thickness of the TiO_2 high-*k* dielectric layer used. There was little hysteresis in bias voltage charging and discharging between successive cycles, producing more consistent device characteristics and operation.

Future work will investigate the use of other high-*k* dielectric materials, different backplate topologies and materials, and modeling of charge migration in the PET and high-*k* layers.

Acknowledgments

The authors would like to thank Mr. Michael O'Shea and Mr. Timothy Power in the mechanical workshop in the Department of Electrical and Electronic Engineering, UCC, and Dr. Conor O'Mahony in the Tyndall National Institute, UCC, for their contributions to the manufacture of the devices used in this work.

References

[1] T.H. Gan, D.A. Hutchins, D.R. Billson and D.W. Schindel, "The use of broadband acoustic transducers and pulse-compression techniques for air-coupled ultrasonic imaging", *Ultrasonics*, vol. 39, pp.181-194, 2001.

[2] E. Blomme, D. Bulcaen, F. Declercq, "Air-coupled ultrasonics NDE: experiments in the frequency range 750 kHz – 2 MHz", *NDT&E International*, vol. 35, pp.417-428, 2002.

[3] A. Turo, J. Salazar, J.A. Chavez, H.B. Kichou, T.E. Gomez, F. Montero de Espinosa and M.J. Garcia-Hernandez, "Ultra-low noise front-end electronics for air-coupled ultrasonic non-destructive evaluation", *NDT&E International*, vol. 36, pp.93-100, 2003.

[4] W.M.D. Wright, O.M. Doyle and C.T. Foley, "Multi-channel data transfer using air-coupled capacitive ultrasonic transducers", *IEEE International Ultrasonics Symposium*, 2006, pp.1805-1808.

[5] J. Hietanen. J. Stor-Pellinen and M. Luukkala, "A model for an electrostatic ultrasonic transducer with a grooved backplate", *Meas. Sci. Technol.*, vol. 3, pp. 1095-1097, 1992.

[6] H. Carr and C. Wykes, "Diagnostic measurements in capacitive transducers", *Ultrasonics*, vol. 31, pp.13-20, 1993.

[7] D.W. Schindel, D.A. Hutchins, L. Zou, and M. Sayer, "The design and characterization of micromachined air-coupled capacitance transducers", *IEEE Trans. UFFC*, vol. 42, pp. 42-50, 1995.

[8] A. Schroder, S. Harasek, M. Kupnik, M. Wiesinger, E. Gornik, E. Benes and M. Groschl, "A capacitance ultrasonic transducer for high-temperature applications", *IEEE Trans. UFFC*, vol.51, pp.896-907, 2004.

[9] K. Suzuki, K. Higuchi and H. Tanigawa, "A silicon electrostatic ultrasonic transducer", *IEEE Trans. UFFC*, vol. 36, pp. 620-627, 1989.

[10] S.G. McSweeney and W.M.D. Wright, "HfO_2 high-k dielectric layers in air-coupled capacitive ultrasonic transducers", *IEEE International Ultrasonics Symposium*, 2011, paper no. 906 (in press).